Inorganic Chemistry

ARTICLE

pubs.acs.org/IC

Low Temperature Neutron Diffraction Studies in $[Mn_3(suc)_2(ina)_2]_n$: An Homometallic Molecular 3D Ferrimagnet

Oscar Fabelo,*[†,‡] Laura Cañadillas-Delgado,[†,‡] Inés Puente Orench,[†,‡] J. Alberto Rodríguez-Velamazán,[†,‡] Javier Campo,[†] and Juan Rodríguez-Carvajal[‡]

[†]Instituto de Ciencia de Materiales de Aragón (ICMA), CSIC-Universidad de Zaragoza, C/Pedro Cerbuna 12, E-50009, Zaragoza, Spain

[‡]Institut Laue-Langevin, Grenoble, 6 rue Jules Horowitz, B.P. 156, 38042 Grenoble Cedex 9, France

Supporting Information

ABSTRACT: Neutron diffraction techniques have been used to determine the low temperature crystal structure and to shed light on the magnetic behavior of the $[Mn_3(suc)_2(ina)_2]_n$ (*suc* = succinate and *ina* = isonicotinate) complex. The ferromagnetic signal observed below $T_c \approx 5$ K in this compound is due to a noncompensation of homometallic spins in the 3D framework. The Mn(II) magnetic moments obtained from neutron diffraction refinements are slightly lower than those observed for isolated Mn(II) ions; this can be due to covalent spin delocalization or geometrical magnetic fluctuations. A small discrepancy between the value of the magnetic moments of each Mn(II) site is also observed [Mn(1) 4.1(2) μ_B and the Mn(2) 3.9(1) μ_B]. These differences between the theoretical and observed manganese magnetic moments are not unexpected in this large spin metal complex, and qualitatively reasonable given the synergistic interaction between the metal ions through oxo-bridge. The competition among different interactions, principally those covalent through organic ligands and dipolar interaction, drive to a final 3D ferrimagnetic order.

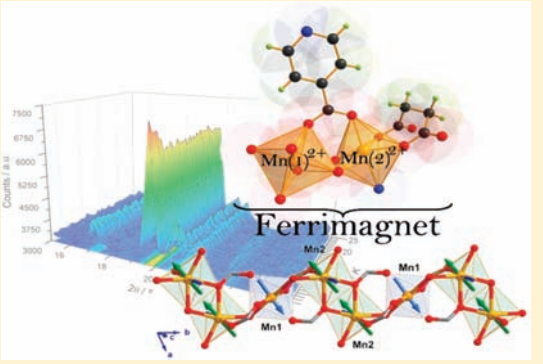

INTRODUCTION

The research on ferrimagnetic systems of metal complexes built up from heterospin systems is well represented by numerous compounds in the field of molecular magnetic materials.[1] These systems are usually synthesized using the well-known chemistry of Schiff base ligands.[2] For such compounds, the long-range ferrimagnetic order arises from the noncompensation of the antiferromagnetically coupled spin moments. The number of three-dimensional (3D) homometallic complexes with ferrimagnetic behaviors previously reported is scarce because only one kind of spin is present, and therefore the noncompensation of the individual spin moments must be achieved through geometric and/or symmetry restrictions.[3] The ordering in these systems typically indicates higher-dimensionality, that is, interchain or interlayer interactions. The role of the weak interactions, as dipolar and next nearest neighbor interactions, and single ion anisotropy, are extremely important to reach a long-range magnetic order. The control of these interactions is the major hurdle for most material architectures. Therefore, an in depth structural and magnetic study is required to understand the physical and chemical factors that govern the exchange coupling between homometallic paramagnetic centers and, as consequence, produce long-range homometallic molecular ferrimagnets.

A compound which presents this interesting magnetic behavior, built up from self-assembly procedure, is the previously reported $[Mn_3(suc)_2(ina)_2]_n$ (with *suc* = succinate and *ina* = isonicotinate, see Scheme 1, left and right, respectively).[4] The structure of this compound was determined by single crystal X-ray diffraction at room temperature (RT),[4] showing that it crystallizes in the $P\bar{1}$ space group with lattice parameters $a = 7.649(3)$ Å, $b = 8.916(3)$ Å, $c = 9.472(3)$ Å, $\alpha = 68.858(5)$, $\beta = 85.627(5)$, and $\gamma = 67.227(5)°$.[4] It can be described with two crystallographically independent Mn(II) centers, forming a regular chain along the *b*-axis, involving μ-oxo bridges from succinate ligands and two *syn-syn* carboxylate bridges, from succinante and isonicotinate ligands. Each chain is linked by two adjacent neighbor-chains through *anti-syn* and *anti-anti* carboxylate bridges, giving rise to a

Scheme 1

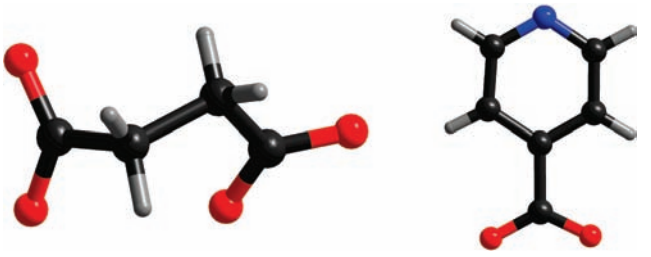

Received: March 30, 2011
Published: July 07, 2011

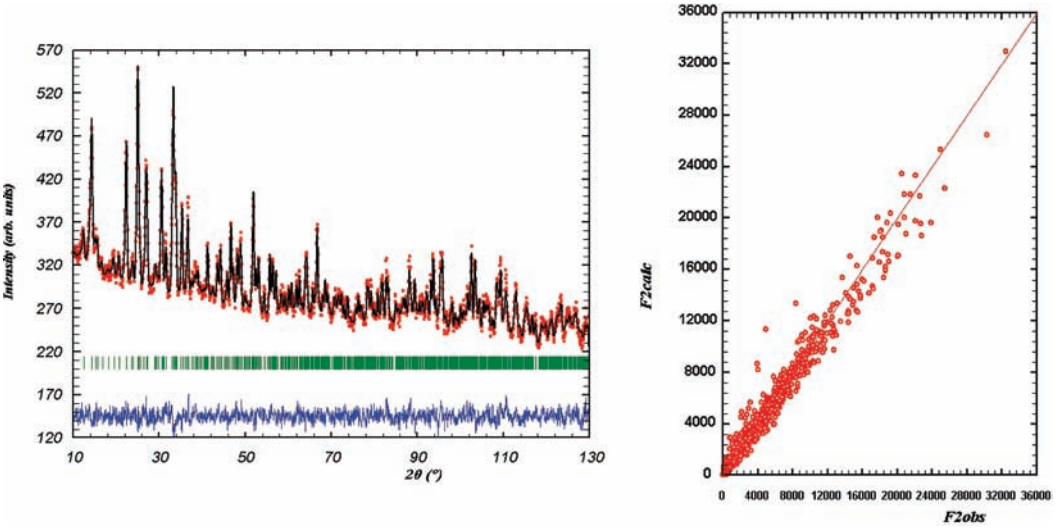

Figure 1. Neutron diffraction pattern of $[Mn_3(suc)_2(ina)_2]_n$ compound collected at 25 K using the D1A instrument with λ = 1.90761 Å (left) and observed vs calculated square structure factors plot for D15 instrument (right). The refinement has been done in the space group $P\bar{1}$ with the associated cell parameters a = 7.5948(4) Å, b = 8.8661(4) Å, c = 9.4481(4) Å, α = 67.764(3)°, β = 84.773(4)°, and γ = 67.282(3)°, with the following statistics χ^2 = 0.83 and R_B= 7.51% for D1A and R_F = 8.12% for D15.

$[Mn_3(suc)_2]_n^{2-}$ rigid layer parallel to the *ab*-plane (Supporting Information, Figure 1S left). The 3D structure is reached through the skeleton of the *ina* ligand, which drives to a pillared system with a *AA* packing mode along the *c* direction with the interlayer distances of about 9.47 Å, (between Mn(1) and Mn(1)^a (a) = x, y, $-1+z$; see Supporting Information, Figure 1S right).

The previous magnetic measurements reveal,[4] at RT, a $\chi_M T$ value (11.85 cm^3 mol^{-1} K) which corresponds to an effective magnetic moment μ_{eff} [= $(8\ \chi T)^{1/2}$] of 5.56 μ_B/Mn(II), consistent with the value of 5.92 μ_B/Mn(II) expected for a magnetically isolated high-spin Mn(II) (S = 5/2) ion with g = 2.00. The $\chi_M T$ values decrease with the temperature down to a minimum (5.94 cm^3 mol^{-1} K) at 20 K. Below this temperature, $\chi_M T$ increases rapidly up to a very high value of 47.14 cm^3 mol^{-1} K at 4.5 K. Upon further cooling, $\chi_M T$ decreases again reaching a value of 29.60 cm^3 mol^{-1} K at 2 K. The sudden increase of $\chi_M T$ at 20 K indicates the presence of ferromagnetic (F) interaction due to the noncancellation of all homometallic spins. The magnetic order was confirmed by the alternating current (ac) magnetic susceptibility and the field-cooled (FC) and zero-field-cooled (ZFC) magnetization measurements which are coincident in the presence of a ferromagnetic phase transition at 5 K. This striking result shows the magnetic order as a consequence of a noncompensated antiferromagnetic (AF) coupling, and therefore a ferrimagnetic behavior is possible. An alternating chain with two interactions, J_1 and J_2, between different exchange couplings was modeled,[4] according with the previous report by Abu-Youssef et al.,[5] where J_1 represents the interaction between Mn(1) and Mn(2) and J_2 between two Mn(2) ions. To take into account the interchain interaction, an extra zJ' parameter was included in the data refinement. It deserves to be noted that a more realistic 3D model is not available. The two different Mn···Mn intrachain distances are 3.708 and 3.530 Å from Mn(1)···Mn(2) and from Mn(2)···Mn(2)^b [(b) = 1 − x, 3 − y, 1 − z], respectively, and the angles Mn(1)−O−Mn(2) and Mn(2)−O−Mn(2)^b are 113.5 and 103.6°, respectively. The shortest Mn···Mn interchain distance involves a succinic carboxylate bridge with a distance of 4.292(2) Å. Therefore, based on the previous result, a competition between F and AF interaction is possible, but even with these results it is not difficult to draw a model where the global exchange coupling gives rise to a strictly AF system.

In the present paper, we report powder and single crystal neutron diffraction studies on $[Mn_3(suc)_2(ina)_2]_n$ compound aiming to refine the crystal structure at low temperature and to determine the magnetic structure in the ordered phase which will shed light on the magnetic conformation that produces a noncompensation of the individual spin moments in this homometallic system.

EXPERIMENTAL SECTION

Materials. Single crystal and powder samples of $[Mn_3(suc)_2(ina)_2]_n$ were prepared following the procedure described by Zeng et al.[4] Reagents and solvents used in the syntheses were purchased from commercial sources and used without further purification. The organic ligands were used without deuteration.

Neutron Diffraction Experiments. Neutron powder diffraction experiments were performed using the D1A, D20, and D1B instruments at the Institut Laue-Langevin, (Grenoble, France) working, respectively, at 1.911 Å, 2.405 Å, and 2.521 Å wavelength. Graphite filters between the monochromator and the sample significantly reduce higher-order wavelength contamination in D20 and D1B diffractometers.

The sample was contained in a Ø 6 mm cylindrical vanadium-can inside an Orange Cryostat (vanadium-tailed). The high resolution neutron pattern (D1A) was collected at 25 K in an angular range of $0 \le 2\theta \le 157.95$ by merging the data obtained by step scans ($\Delta 2\theta$ = 0.05°) of the block of 25 high efficiency counters separated 6.0°. The high-flux neutron patterns (D20) were collected at 2 and 25 K. A neutron thermodiffractogram between 2 and 300 K, with a heating rate of 2 K/min, was also measured using the high-flux D1B diffractometer.

The data reduction (including the application of some basic operations as those related with the addition of several patterns or detector efficiency corrections) was done with the LAMP software.[6]

The single crystal neutron diffraction experiments were carried out at D15 instrument at Institut Laue Langevin on a non deuterated single crystal of 5 × 3 × 2 mm dimensions. The instrument, provided with a closed-cycle cryostat, was used in the four-circle configuration with a

dx.doi.org/10.1021/ic200655y |*Inorg. Chem.* 2011, 50, 7129–7135

wavelength of 1.173 Å. The COLL5 program[7] was used to integrate the ω-scans and to correct them from the Lorentz factor. The absorption corrections were done using the DATAP program,[8] using an estimated total neutron absorption coefficient of 1.72 cm^{-1}, essentially due to the large incoherent scattering of the hydrogen atoms. The integrated intensities were collected at 25 K (above T_c), where only nuclear scattering was present, and at 2 K (below T_c) where also a magnetic contribution, due to the ordered magnetic moments, was present.

Nuclear and magnetic structures were refined using a multipattern approach based on the simultaneous Rietveld and Integrated Intensities refinements, for powder and single crystal data, respectively, implemented in the FullProf suite of programs.[9] The nuclear structure at low temperature was refined from an initial model derived from single crystal X-ray diffraction data collected at RT.[4]

RESULTS

Nuclear Structure at 25 K. With the main objective of obtaining an accurate structural model, a high resolution neutron diffractogram was recorded at 25 K at the D1A instrument and analyzed together with 1084 independent Bragg reflections collected on D15 at the same temperature through a multipattern procedure [see Figure 1]. The determination of the cell parameters at 25 K, as well as the atomic position refinement, was carried out without any restriction. Because of the possible bonding effects, special care was taken with the C−H bond distances, considering the well-known difference in hydrogen positions observed by X-ray and neutron scattering. To not over parameterize the model, the thermal parameters were considered isotropic (Biso) for all atoms, except for the hydrogen atoms which were refined with an anisotropic model. A total of 163 parameters were refined, of which 146 parameters affect the integrated intensities. The best refinements to the experimental data at 25K are shown at Figure 1 (χ^2 = 0.83 and R_B = 7.51% for D1A and R_F = 8.12% for D15). The refined structure is closely similar to that observed in X-ray measurements at RT. A small compression of the cell parameters together with a reorganization of the organic ligand, both effects due to the low temperature, and in particular the correct positioning of H atoms, because of the use of neutrons, are the principal differences observed. Supporting Information, Figure 2S and Table 1S show and list, respectively, the small structural changes and the structural parameters.

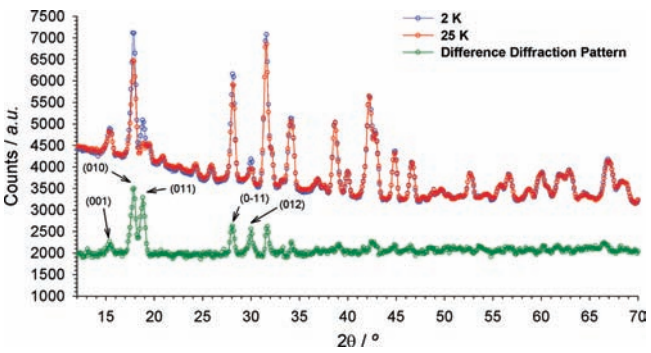

Figure 2. Neutron powder patterns of $[Mn_3(suc)_2(ina)_2]_n$ compound, collected at 2 and 25 K using D20 powder diffractometer, in blue and red, respectively. The difference diffraction pattern with some characteristic reflections is represented in green. The difference between both diffraction patters is due to the contribution of magnetic phase.

Magnetic Structure at 2 K. On the basis of the results of magnetic susceptibility and magnetization studies of the homometallic ferrimagnetic compounds $[Mn_3(suc)_2(ina)_2]_n$,[4] elastic neutron scattering experiments were undertaken at low temperature with the goal of revealing the magnetic structure of the ferrimagnetic phase ($T_c \approx 5K$) of this specific Mn(II) homometallic system.

The neutron thermodiffractogram taken at D1B shows an increase of intensity below T_c only in some nuclear Bragg peaks which is a fingerprint of the appearance of some magnetic order below 5.5 K. The difference between 2 K and 25 K diffraction patterns taken at D20 presents similar behavior as can be observed in Figure 2. The temperature dependence of the integrated intensity for the (011) and (012) reflections collected at the D15 instrument is depicted in Supporting Information, Figure 3S. All these magnetic contributions to the diffractograms observed at low temperature in D1B, D20, and D15 can be indexed with a magnetic propagation vector $\mathbf{k}$ = (0 0 0).

The change in the intensity of some nuclear reflections observed in the paramagnetic phase (25−300 K) could be related with small thermal-reorientations of the organic ligands (see Figure 3 and Supporting Information, Figure 4S).

The unit cell parameters, determined from a profile matching of powder neutron diffraction patterns, are in good agreement with those parameters determined by the single-crystal diffraction employing X-ray and neutron measurements.

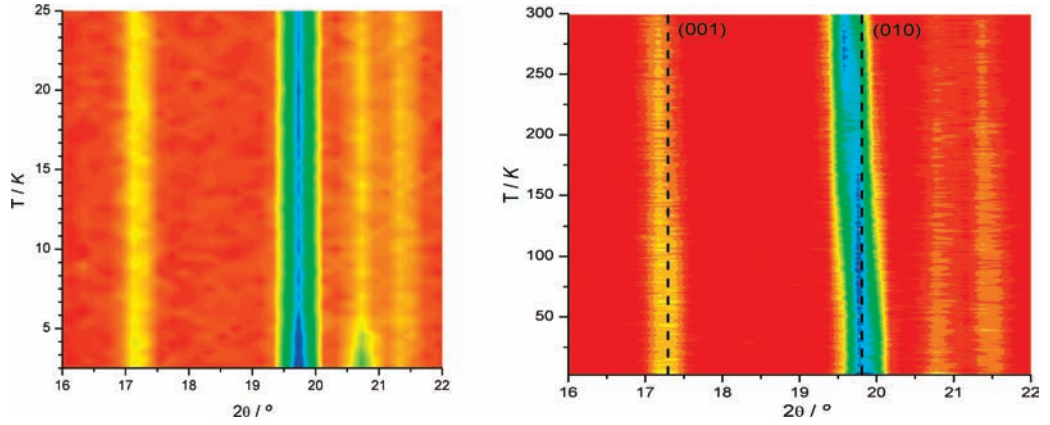

Figure 3. Mesh plot of $[Mn_3(suc)_2(ina)_2]_n$ compound collected at D1B in the temperature range of 2−25 K, showing the increase of intensity at T_c (ca. 5.5 K) because of the occurrence of magnetic order (left). Mesh plot of $[Mn_3(suc)_2(ina)_2]_n$ compound collected at D1B in the temperature range of 2−300 K for two selected reflections, showing the regularity of the nuclear phase as a function of the temperature (right). The slight displacement of the nuclear reflections is due to cell parameter contraction (dashed lines are drawn to guide the eyes).

dx.doi.org/10.1021/ic200655y |Inorg. Chem. 2011, 50, 7129–7135

To determine the possible magnetic structures compatible with the symmetry of the crystal structure of $[Mn_3(suc)_2(ina)_2]_n$ we have used the representational analysis techniques described by Bertaut.[10]

The propagation vector group G_k (little group) coincides with the space group $P\bar{1}$. The two 1-dimensional irreducible representations (irreps) of the group G_k, Γ_1 and Γ_2, and a set of basis vectors for each irrep are trivial, and we verified the calculations using the program BASIREPS (included in the FullProf Suite).[11] The irreducible representations and basis vectors are shown in Table 1. The magnetic representation Γ_M for each magnetic site [Wyckoff position 1*f* for Mn(1) and 2*i* for Mn(2)] can be decomposed as direct sum of irreps by applying the great orthogonality theorem. Each irrep Γ_1 and Γ_2 appears 3 times for the site 2*i* whereas for the site 1*f* only Γ_1 is present

$$\Gamma_{1f} = 3\Gamma_1 \quad (1)$$

$$\Gamma_{2i} = 3\Gamma_1 \oplus 3\Gamma_2 \quad (2)$$

Table 1. Irreducible Representations (irreps) Γ of the Little Group $G_k = P\bar{1}$ [a]

irreps		*E*	*−1*
Γ_1		1	1
Γ_2		1	−1
basis vectors		*x, y, z*	*−x,−y, −z*
Γ_1	Mn(1*f*)	{(100), (010), (001)}	
	Mn(2*i*)	{(100), (010), (001)}	{(100), (010), (001)}
Γ_2	Mn(1*f*)	{(100), (010), (001)}	
	Mn(2*i*)	{(100), (010), (001)}	{(−100), (0−10), (00−1)}

[a] Basis vectors of the 2 irreducible representations for the sites Mn(1*f*) = 0.5, 0, 0.5 and Mn(2*i*) = 0.2970, 0.4535, 0.4938.

Irrep Γ_1 is related with an independent ferromagnetic configuration of spins at site 1*f* and 2*i* whereas Γ_2 represents an antiferromagnetic order for the 2*i* site. The symmetry analysis cannot give information about the phase existing between both magnetic sublattices.

The magnetic moment for site 1*f* is obtained from the basis vectors as $\mathbf{m}_{1f}$ = (u, v, w) and the magnetic moments of the two sublattices of site 2*i* as $\mathbf{m}_{2i}$ (1) = (p, q, r) and $\mathbf{m}_{2i}$ (2) = (p, q, r) for irrep Γ_1 and as $\mathbf{m}_{2i}$ (1) = (p, q, r) and $\mathbf{m}_{2i}$ (2) = (−p, −q, −r) for irrep Γ_2. In both cases there are six degrees of freedom (u, v, w, p, q, r) for the magnetic structure. The Shubnikov group corresponding to Γ_1 is $P\bar{1}$ and that corresponding to Γ_2 is $P\bar{1}'$.

If we consider that both sublattices are ordered, the magnetic structure can only be described by irrep Γ_1. This is because Γ_2 is not contained in Γ_{1f}. If the site 2*i* was ordered according to Γ_2 necessarily the site 1*f* would be disordered or the center of symmetry would disappear by a symmetry breaking to *P*1. The relative orientation of the magnetic moments of the sites 2*i* and 1*f* is not fixed by symmetry and should be determined by refining the neutron diffraction patterns. The general result will correspond to a noncollinear structure if $\mathbf{m}_{1f}$ is not parallel to $\mathbf{m}_{2i}$.

The multipattern magnetic refinements at 2 K were carried out with the powder neutron diffraction pattern collected at D20 diffractometer, operated in a medium resolution configuration, combined with 77 low Bragg angle reflections collected at the same temperature on D15. The solid line in Figure 4, left represents the calculated fit for the best refinements (χ^2 = 9.56 and R_B= 5.34% for D20 and R_F = 3.56% for D15) of the diffractograms taken at 2 K in D20 and corresponding with the first model explained above. The Figure 4, right represents the observed and calculated squared structure factors obtained from the D15 measurement.

The magnetic moments of the Mn(II) ions determined by the refinement of the D20−D15 data at 2 K are Mn(1*f*) = 4.1(2) μ_B

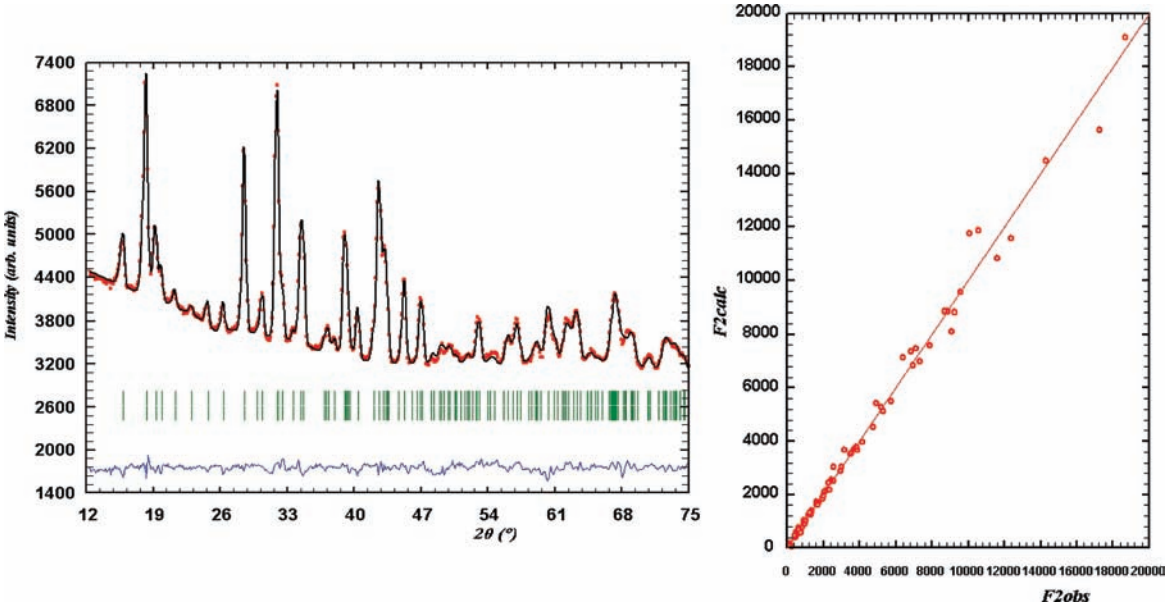

Figure 4. Neutron diffraction patterns collected at 2 K at D20 (left) and observed vs calculated square structure factors plot collected at D15 (right). The data refinement with the irreducible representations Γ_1 gives rise to the following agreement factors χ^2 = 9.56 and R_B = 5.34% for D20 and R_F = 3.56% for D15.

dx.doi.org/10.1021/ic200655y |*Inorg. Chem.* 2011, 50, 7129–7135

and Mn(2*i*) = 3.9(1) μ_B and are listed in Table 2. The spin moment of the Mn(1*f*) atoms is pointing nearly to a vertex of the octahedral environment corresponding with Mn(1)−O(6) bond. It deserves to be noted that Mn(1*f*) atoms show a slightly distorted octahedral environment, while the Mn(2*i*) environment is far from being a perfect octahedron. The magnetic moment of Mn(2*i*) is nearly contained in a distorted equatorial plane, built up from the carboxylate oxygen atoms [O(3), O(5), O(4)^c and O(5)^b with (*c*) = $-x$, 3 − *y*, 1 − *z*][see Figure 5].

The uncompensated ferrimagnetic moment (μ_f) of the Mn(II) sublattices, calculated as vector sum of the magnetic moments obtained from the neutron measurement at 2K, is 4.78 μ_B (see Figure 5c). This value is similar to that observed at the saturation value, with 50000 Oe applied field, in the magnetization versus magnetic field isotherms at 2K (ca. 5.2 μ_B obtained for three Mn(II)). Comparing the theoretical value of 5.00 μ_B (for Mn(II) ion *S* = 5/2 and Landé factor *g* = 2.00) with that obtained in our experiment, we observe an about 18% and 22% of reduction, for Mn(1*f*) and Mn(2*i*), respectively. These reductions of magnetic moment could be interpreted as a result of the geometrical distortion present in this system (larger in the case of 2*i* sites) which could induce some magnetic anisotropy or because of covalent delocalization of the magnetic moment along the nonmagnetic ligands surrounding each Mn(II) ion.[12] It deserves to be noted that the present neutron diffraction experiments give only information about the magnetic moment resident on the Mn(II) sites and not out of them.

Table 2. Magnetic Moment Components Determined for Each Mn(II) Site[a]

	M_a	M_b	M_c	M_{total}
Mn(1*f*)	3.7(2)	0.2(4)	1.5(2)	4.1(2)
Mn(2*i*)	−3.3(2)	−1.3(3)	0.8(2)	3.9(1)

[a] The components (in μ_B) are given with respect to the unit vectors along **a**, **b** and **c**.

DISCUSSION

From a magnetic point of view a topological exchange coupling model can be sketched taking into account the different bridges present in $[Mn_3(suc)_2(ina)_2]_n$. Six different exchange couplings between manganese ions can be drawn. The principal ones are those two within the inorganic chain J_1 between Mn(1*f*) and Mn(2*i*) and J_2 between Mn(2*i*) ions (see Figure 5a). Two different Mn···Mn interchain interactons J_3 from Mn(2*i*)···Mn(1*f*)^d [with (*d*) = −1 + *x*, 1 + *y*, *z*] and J_4 from Mn(2*i*)···Mn(2*i*)^c are also present with a distance of 6.170(2) and 4.292(2) Å, respectively, giving rise to a layer motif extended along the *ab*-plane. The last interactions J_5 and J_6 are through the skeleton of the *ina* ligand from Mn(1*f*)···Mn(2*i*)^a and Mn(2*i*)···Mn(2*i*)^a [with (*a*) = *x*, *y*, −1 + *z*], with the shorter interlayer distances of about 9.4 Å, and producing the final 3D

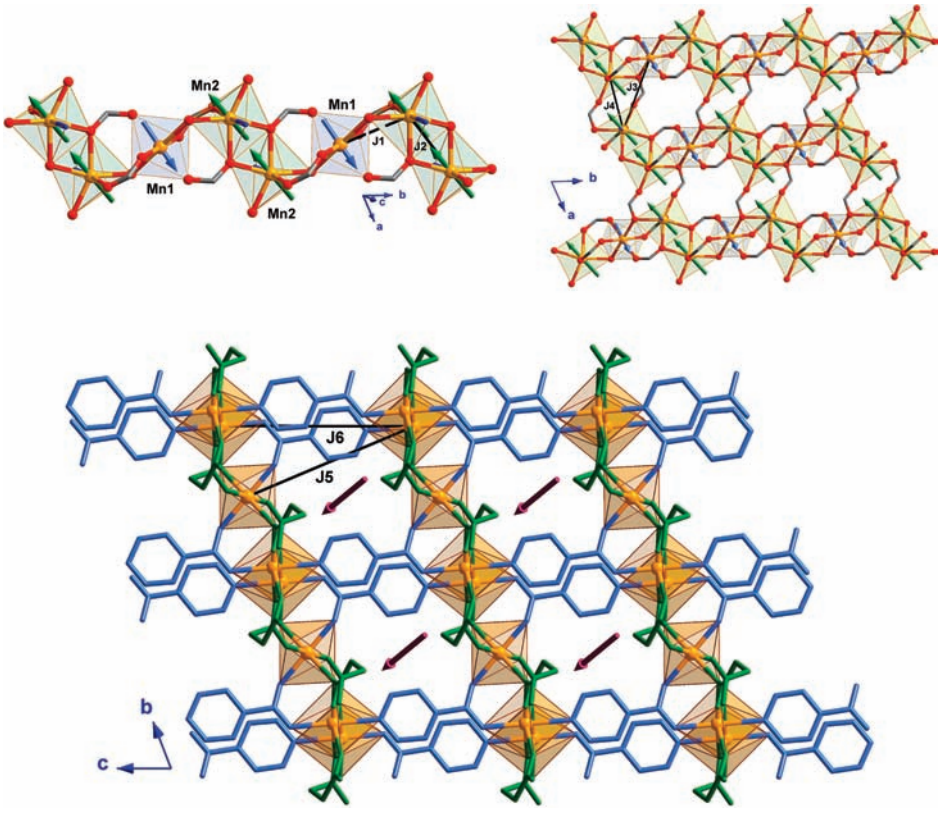

Figure 5. (a) View along the *b*-axis of a fragment of the crystal structure together with the magnetic moment of each Mn(II) site. (b) Perspective view along the *c*-axis of the inorganic layer together with the magnetic moment of each magnetic site. For clarity only the carboxylate groups of *suc* and *ina* ligands have been drawn in (a) and (b). (c) Perspective view of $[Mn_3(suc)_2(ina)_2]_n$ compound together with a vector representing the total magnetic moment (dark red) as result of the magnetic coupling between different Mn(II) atoms. The total magnetization per molecular unit is calculated as **M** = ($\mathbf{m}_{1f}$ + 2$\mathbf{m}_{2i}$) ≈ (−2.9, −2.4, 3.1). The hydrogen atoms of the *suc* and *ina* ligands have been omitted for clarity. The different exchange couplings mentioned in the text (J_1−J_6) have been represented as black sticks for a better understanding of the text.

dx.doi.org/10.1021/ic200655y |*Inorg. Chem.* 2011, 50, 7129–7135

motif. An interpretation of the magnetic properties as a function of the different bridges present in the crystal structure can be derived from the magnetic model obtained from neutron diffraction. The schematic magnetic interactions within the chain present the alternating sequence F-AF-AF-F (with F and AF as ferromagnetic and antiferromagnetic interactions, respectively), F between Mn(2*i*) ions (J_2) and AF between Mn(1*f*) and Mn(2*i*) ions (J_1). The AF coupling between Mn(1*f*)···Mn(2*i*) involves three different bridges; one μ-oxo with an angle of 113.5(1)°, which is predicted to be AF,[13] and two *syn-syn* carboxylate bridges, that would cause an AF coupling, as supported by a large number of magneto-structural studies.[14] Nevertheless, the presence of different bridges can add or counterbalance their effects. This problem was treated by Nishida et al.[15] and McKee et al.[16] These two situations are referred to as orbital complementarity and counter-complementarity, respectively. On the other hand, the coupling between Mn(2*i*) ions through the double μ-oxo bridges has been characterized as ferromagnetic. The superexchange angle Mn(2i)−O(5)−Mn(2i) is 103.6(6)° and the distance between two adjacent Mn(2*i*) is 3.5303(13) Å.

The interchain coupling through 1,3-carboxylate bridges promotes the parallel spin configuration when this bridge acts in *anti-syn* manner (J_4) [Mn(2*i*)-OCO-Mn(2*i*)^c] while it promotes antiparallel spin configuration when acting in *anti-anti* conformation (J_3) [Mn(1*f*)-OCO-Mn(2*i*)^c]. The interlayer coupling, through the *ina* ligands, is expected to promote a weak AF interaction (J_5 and J_6).[17] The possibility of a two-dimensional ordering was discarded based on the neutron diffraction measurements below the order temperature.

The 3D magnetic ordering could come from the competition between the covalent bridge exchange interaction, which could be enhanced by a possible spin delocalization,[12] and the dipolar interaction between the adjacent layers separated by *ina* ligands over a distance of about 9.4 Å.[18] The dipolar interaction is proportional to R^{-3}, R being the distance between the magnetic centers, while the covalent bridge exchange interaction through bonds is expected to be negligible as it follows a R^{-10} dependence.[19] If the moments are large enough, the dipolar interaction could become more important in the molecular magnet at a large distance, and although it might be rather weak, it may be strong enough to induce 3D magnetic ordering like this which has been observed previously in clusters,[20] chains,[21] and layers.[18−22]

The above neutron diffraction results, therefore, confirm the 3D magnetic structure which shows a regular staking in an *AA* sequence and the fact that ferrimagnetic behavior is promoted by noncompensation of the magnetic moment of the different magnetic ions present in the crystal.

CONCLUSION

In this work we have refined the crystal structure of $[Mn_3(suc)_2(ina)_2]_n$ compound from neutron diffraction data at 25 K. It shows slight differences in the ligand conformation compared with those data obtained with X-ray at RT and has allowed the localization of hydrogen atoms. The 25 K structural model has been used as starting point for the refinement of the magnetic structure. On the basis of a symmetry analysis, only the Γ_1 irreducible representation is possible for the magnetic ordering. This representation is that effectively found for both sites simultaneously. It fits very well the experimental data. The magnetic interactions give rise to a noncollinear ferrimagnetic structure. The ferrimagnetic behavior is the result of a competition between the different exchange coupling interactions, principally the intrachain ones. The 3D magnetic ordering might come from the competition between the covalent bridge exchange interaction and the dipolar interaction between inorganic layers separated by *ina* ligands.

The difference of magnetic moment determined for each Mn(II) site compared with those observed in the pure ionic configuration can be due to a combination of geometrical distortion and/or strong covalence effects.

ASSOCIATED CONTENT

Supporting Information. Further details are given in Table 1S and Figures 1S−4S. This material is available free of charge via the Internet at http://pubs.acs.org.

AUTHOR INFORMATION

Corresponding Author
*E-mail: fabelo@ill.fr.

ACKNOWLEDGMENT

The present work was partly funded through projects MAT2009-13977-C03 (MOLCHIP), MAT2011-M4E2, MAT2010-16981, MAT2007-61621, MAT2007-60660, and the Consolider-Ingenio projects CSD2007-00010 and CTQ2007-61690 from the Spanish MICINN. We are grateful to the ILL and Spanish-CRG instruments by the neutron beam-time allocated.

REFERENCES

(1) (a) Miller, J. S.; Manson, J. *Acc. Chem. Res.* **2001**, *34*, 563. (b) Tamaki, H.; Zhong, Z. J.; Matsumoto, N.; Kida, S.; Koikawa, M.; Achiwa, N.; Hashimoto, Y.; Okawa, H. *J. Am. Chem. Soc.* **1992**, *114*, 6974. (c) Coronado, E.; Galán-Mascarós, J. R.; Martí-Gastaldo, C. J. *J. Mater. Chem.* **2006**, *16*, 2685. (d) Ribas, J.; Escuer, A.; Monfort, M.; Vicente, R.; Cortes, R.; Lezama, L.; Rojo, T.; Goher, M. A. S. *Magnetism: Molecules to Materials II: Molecule-Based Materials*; Millar, J. S., Drillon, M., Eds.; Wiley-VCH: Weinheim, Germany, 2001. (e) Wang, T.-W.; Wang, J.; Ohkoshi, S.; Song, Y.; You, X.-Z. *Inorg. Chem.* **2010**, *49* (17), 7756.

(2) (a) Miyasaka, H.; Matsumoto, N.; Re, N.; Gallo, E.; Floriani, C. *Inorg. Chem.* **1997**, *36* (4), 670. (b) Visinescu, D.; Toma, L. M.; Lloret, F.; Fabelo, O.; Ruiz-Pérez, C.; Julve, M. *Dalton Trans.* **2008**, 4103. (c) Miyasaka, H.; Okawa, H.; Miyazaki, A.; Enoki, T. *J. Chem. Soc., Dalton Trans.* **1998**, 3991. (d) Wen, H.-R.; Wang, C.-F.; Li, Y.-Z.; Zuo, J.-L.; Song, Y.; You, X.-Z. *Inorg. Chem.* **2006**, *45* (18), 7032. (e) Yoo, H. S.; Ko, H. H.; Ryu, D. W.; Lee, J. W.; Yoon, J. H.; Lee, W. R.; Kim, H. C.; Koh, E. K.; Hong, C. S. *Inorg. Chem.* **2009**, *48* (13), 5617.

(3) (a) Konar, S.; Mukherjee, P. S.; Zangrando, E.; Lloret, F.; Chaudhuri, N. R. *Angew. Chem., Int. Ed.* **2002**, *41*, 1561. (b) Guillou, N.; Pastre, S.; Livage, C.; Férey, G. *Chem. Commun.* **2002**, 2358. (c) Chen, H. J.; Mao, Z. W.; Gao, S.; Chen, X. M. *Chem. Commun.* **2001**, 2320–2321. (d) Wang, R.; Gao, E.; Hong, M.; Gao, S.; Luo, J.; Lin, Z.; Han, L.; Cao, R. *Inorg. Chem.* **2003**, *42*, 5486. (e) Zeng, M.-H.; Wu, M.-C.; Liang, H.; Zhou, Y.-L.; Chen, X.-M.; Ng, S.-W. *Inorg. Chem.* **2007**, *46*, 7241.

(4) Zeng, M.-H.; Wu, M.-C.; Liang, H.; Zhou, Y.-L.; Chen, X.-M.; Ng., S.-W. *Inorg. Chem.* **2007**, *46* (18), 7241.

(5) Abu-Youssef, M. A. M.; Drillon, M.; Escuer, A.; Goher, M. A. S.; Mautner, F. A.; Vicente, R. *Inorg. Chem.* **2000**, *39*, 5022.

(6) (a) *LAMP, the Large Array Manipulation Program*; http://www.ill.fr/data_treat/lamp/lamp.html. (b) Richard, D.; Ferrand, M.; Kearley, G. J. *J. Neutron Res.* **1996**, *4*, 33.

(7) Lehmann, M. S.; Larsen, F. K. *Acta Crystallogr.* **1974**, *A30*, 580.

(8) Coppens, P. *Crystallographic Computing*; Ahmed, F. R., Ed.; Munksgaard International Booksellers and Publishers Ltd.: Copenhagen, Denmark, 1979; pp 255−270.

(9) (a) Rodríguez-Carvajal, J.*FULLPROF program*; Institut Laue-Langevin (ILL), 2009 (b) Rodríguez-Carvajal, J. *Physica* **1993**, *B192*, 55 (The programs of the FullProf Suite and their corresponding documentation can be obtained from the web at http://www.ill.eu/sites/fullprof/).

(10) Bertaut, E. F. In *Magnetism*; Rado, G. T. Shul, H., Eds.; Academic: NewYork, 1963; Vol.III, Chapter 4.

(11) Rodríguez-Carvajal, J. *BasIreps program*; Institut Laue-Langevin (ILL), 2009

(12) (a) Luzón, J.; Campo, J.; Palacio, F.; Mc Intyre, G. J.; Millán., A. *Phys. Rev. B.* **2008**, *78*, 054414(9). (b) Campo, J.; Luzón, J.; Palacio, F.; Mc Intyre, G. J.; Millán, A.; Wildes., A. R. *Phys. Rev. B.* **2008**, *78*, 054415(10).

(13) Ruiz, E.; Alvarez, S.; Alemany, P. *Chem. Commun.* **1998**, 2767.

(14) (a) Cano, J.; Demunno, G.; Sanz, J.; Ruiz, R.; Lloret, F.; Faus, J.; Julve, M. *J. Chem. Soc., Dalton Trans.* **1994**, 3465 and references cited therein. (b) Hong, C. S.; Do, Y. *Inorg. Chem.* **1997**, *36*, 5684. (c) Oshio, H.; Ino, E.; Mogi, I.; Ito, T. *Inorg. Chem.* **1993**, *32*, 5697. (d) Albela, B.; Corbella, M.; Ribas, J.; Castro, I.; Sletten, J.; Stoeckli-Evans, H. *Inorg. Chem.* **1998**, *37*, 788. (e) Hong, C. S.; Son, S.-K.; Lee, Y. S.; Jun, M.-J.; Do, Y. *Inorg. Chem.* **1999**, *38*, 5602. (f) Mukherjee, P. S.; Konar, S.; Zangrando, E.; Mallah, T.; Ribas, J.; Chaudhuri, N. R. *Inorg. Chem.* **2003**, *42*, 2695. (g) Ma, C.; Wang, W.; Zhang, X.; Chen, C.; Liu, Q.; Zhu, H.; Liao, D.; Li, L. *Eur. J. Inorg. Chem.* **2004**, 3522. (h) Cañadillas-Delgado, L.; Fabelo, O.; Pasán, J.; Delgado, F. S.; Lloret, F.; Julve, M.; Ruiz-Pérez, C. *Inorg. Chem.* **2007**, *46*, 7458.

(15) Nishida, Y.; Kida, S. *J. Chem. Soc., Dalton Trans.* **1986**, 2633.

(16) (a) McKee, V.; Zvagulis, M.; Reed, C. A. *Inorg. Chem.* **1983**, *24*, 2914. (b) McKee, V.; Zvagulis, M.; Dagdigian, J. V.; Match, M. G.; Reed, C. A. *J. Am. Chem. Soc.* **1984**, *106*, 4765.

(17) (a) Liu, Y.-H.; Lu, Y.-L.; Tsai, H.-L.; Wang, J.-C.; Lu, K.-L. *J. Solid State Chem.* **2001**, *158*, 315. (b) Yang, B.-P.; Zeng, H.-Y.; Dong, Z.-C.; Mao, J.-G. *J. Coord. Chem.* **2010**, *56* (17), 1513. (c) He, Z.; Wang, Z.-M.; Gao, S.; Yan, C.-H. *Inorg. Chem.* **2006**, *45* (17), 6694.

(18) (a) Kurmoo, M.; Day, P.; Derory, A.; Estournès, C.; Poinsot, R.; Stead, M. J.; Kepert, C. J. *J. Solid State Chem.* **1999**, *145*, 452. (b) Kurmoo, M. *J. Mater. Chem.* **1999**, *9*, 2595. (c) Cano, J.; De Munno, G.; Sanz, J. L.; Ruiz, J. L.; Faus, R.; Lloret, J. F.; Julve, M.; Caneschi, A. *J. Chem. Soc., Dalton Trans.* **1997**, 1915.

(19) Bloch, D. *J. Phys. Chem. Solids* **1966**, *27*, 881.

(20) (a) Morello, A.; Mettes, F. L.; Bakharev, O. N.; Brom, H. B.; Jongh, L. J.; Lu, F.; Fernández, J. F.; Aromí, G. *Phys. Rev. B.* **2006**, *73*, 134406. (b) Affonte, M.; Lasjaunias, J. C.; Wernsdorfer, W.; Sessoli, R.; Gatteschi, D.; Heath, S. L.; Fort, A.; Rettori, A. *Phys. Rev. B.* **2002**, *66*, 064408.

(21) (a) Wynn, C. M.; Gîrtu, M. A.; Brincherhoff, W. B.; Sugiura, K.-I.; Miller, J. S.; Epstein, A. P. *Chem. Mater.* **1997**, *9*, 2156. (b) Ostrovsky, S.; Haase, W.; Drillon, M.; Panissod, P. *Phys. Rev. B.* **2001**, *64*, 134418.

(22) (a) Kurmoo, M. *Chem. Mater.* **1999**, *11*, 3370. (b) Drillon, M.; Panissod, P. *J. Magn. Magn. Mater.* **1998**, *188*, 93.